Physical Sciences Research International
Vol. 3(2), pp. 26-36, June 2015
ISSN: 2437-1300
Full Length Research Paper

Study of the DC-electrical properties of a novel polyvinyl alcohol/Ag hybrid nanocomposites

Eman K. Tawfik[1], Y. H. A. Fawzy[1], M. H. El-Ghazaly[2] and H. A. Ashry[1]*

[1]National Center for Radiation Research and Technology, Nasr-City, Cairo, Egypt.
[2]Physics Department, Faculty of Science, Zagazig University, Egypt.

Accepted 28 May, 2015

ABSTRACT

The present paper investigates a detailed study on the electrical properties of pure PVA and PVA/Ag nanocomposite films. In this concern, PVA/Ag nanocomposites with different contents of inorganic phase of 2 to 8 wt% were prepared by reduction of Ag^+ ions in PVA solution using gamma irradiation with different doses of 15, 25, 50, 75 and 100 kGy. In FTIR analysis proved the formation of chemical bonding/conjugation between the Ag nanoparticles and PVA chains. The dc-electrical conductivity was shown to be function of both Ag concentration and gamma-dose, where its value was shown to increase, up to around 5.3×10^{-9} $S.cm^{-1}$, as a function of Ag concentration, up to about 7.0 wt%, while, it starts decreasing for higher Ag concentration. On the other hand, its value was shown to be decreased as the gamma-dose increased to 50 kGy. For higher dose levels, up to 100 kGy, the conductivity re-increases, again, up to around 6.5×10^{-9} $S.cm^{-1}$.

Keywords: Polyvinyl alcohol**,** silver, nanocomposite, gamma-radiation, dc-electrical conductivity, conduction mechanism, electrometer.

*Corresponding author. E-mail: hashry14@hotmail.com.

INTRODUCTION

Electrical properties of materials have long been of practical importance and theoretical interest. It is well known that electric properties measurements are powerful tools to characterize inorganic semiconductor doped on polymer nanocomposites which give information about electronic properties and help to show the relations between structure and electrical properties of nanocomposites. In this concern, the polyvinyl alcohol (PVA) polymer was chosen as a host matrix due to the advantage of its high mechanical strength, water-solubility, good environmental stability and dopant dependent electrical conductivity.

Polyvinyl alcohol (PVA) is a good insulating material with low conductivity and low dielectric loss, and hence of importance to the microelectronics industry, its electrical conductivity and charge storage capability can be markedly influenced by doping with Ag. The electrical and optical properties of polymers can be suitably modified by the addition of dopant depending on their reactivity with the host matrix. Since Ag^+ is a fast conducting ion in a number of crystalline and amorphous materials, its incorporation within a polymeric system will enhance its electrical performance. Finally, the present paper is a trial to shed further light on the electrical properties of pure PVA and PVA/Ag nanocomposite films.

EXPERIMENTAL

Sample preparations

During the course of the study, PVA/Ag nanocomposite films were prepared. In this concern, 3.0 g of PVA is dissolved in 100 ml of de-ionized water with stirring at 90°C. The freshly prepared $AgNO_3$ solution 0.1 M was added drop wise in aqueous PVA with continuously

stirring for about 2 h to insure the homogeneity of the solution. To stabilize the PVA/$AgNo_3$ against photo reduction the pH-value of the solution was adjusted to 4.0 with an aqueous solution of HNO_3. The solution was casted to glass Petri-dishes and left to dry at room temperature then the resulted films were peeled off. Finally, a set of the prepared polymeric samples were gamma-irradiated, up to 15, 25, 50, 75 and 100 kGy in order to reduce the Ag^+ ions. The content of inorganic phase Ag in the nano-composite films were assured to be 2.0, 3.0, 4.0, 5.0, 6.0, 7.0 and 8.0 wt%, by using X-Ray Fluorescence analysis spectrophotometery Technique (Tawfik et al., in press).

Experimental apparatus

The experimental apparatus is mainly comprised of:

Fourier transform infrared spectroscopy, Jasco–6100

Fourier Transform Infrared spectra, FTIR of Ag/PVA nanocomposites were collected using Jasco Inst., model 6100, Japan in the absorbance mode at a resolution of 4.0 cm^{-1}.

Gamma-cell 220, Excel Co^{60}

Gamma-Irradiation was carried out using the Gamma cell 220 Excel Co^{60} irradiation facility, manufactured by MDS Nordion, Canada, of the National Center for Radiation Research and Technology. The absorbed irradiation dose rate of the γ−cell was measured using National Physical Laboratory (NPL) alanine reference dosimeter. The irradiation dose rate was found to be in the range 8.60 to 8.65 kGy/h along the time of the experiment. A set of test polymeric samples was subjected to different irradiation dose levels of 15, 25, 50, 75, and 100 kGy.

Digital electrometer, Keithley-6517A

The Keithley 6517A offers accuracy and sensitivity and variety of features that simplify measuring high resistances and the resistivity of insulating materials.

Infrared spectroscopic analysis

Infrared (IR) spectroscopic analysis was carried out applying the JASCO FT/IR–6100 FTIR spectrometer. The measurements represent a novel tool for illustration of the composition and nature of bond formation into PVA/Ag nanocomposites (Ghanipour and Dorranian, 2013).

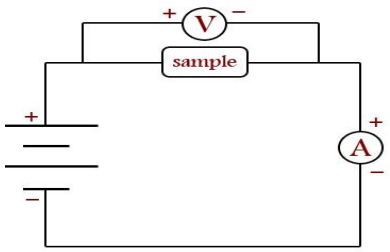

Figure 1. The circuit used for DC-conductivity measurements.

Electrical properties measurements

During the course of the present research work, the dc-conductivity of the prepared samples was studied applying the circuit shown in Figure 1, where variable dc-power supply was used, and the dc-voltage range was chosen to be from 0 up to 200 V, in steps of 10 and 20 V.

RESULTS AND DISCUSSION

Composition and nature of bond formation of PVA/Ag nanocomposites

FTIR spectroscopic analysis of pure PVA

The IR spectrum for pure PVA is shown in Figure 2 and the frequencies of the absorption bands together with their structural assignments are listed in Table 1. The O-H stretching band in the infrared spectrum is by far the most characteristic feature of alcohols and phenols. PVA sample gave very broad and strong band centered at 3330 cm^{-1} as the stretching vibration of hydroxyl group with strong hydrogen bonding as intra-and/or intertype (Ali et al., 2009). Two strong peaks at 2939 and 2866 cm^{-1} are the characteristic bands of asymmetric and symmetric aliphatic C-H stretching respectively. From which, it is clear that two medium bands in the un-saturation region (1732 to 1500 cm^{-1}). The stretching vibrational band of C=O can be seen at 1614 cm^{-1} whereas the characteristic infrared peak of C=C appeared at 1533 cm^{-1}.

The C=O bands were attributed to the carbonyl functional groups due to the residual acetate groups remaining after the manufacture of PVA from hydrolysis of polyvinyl acetate and oxidation during manufacturing and processing while the C=C may be a result of cross-linking results from heating the polymer through sample preparation (Mohri et al., 1995). The values of C=O and C=C indicate that PVA has the same resonating structure

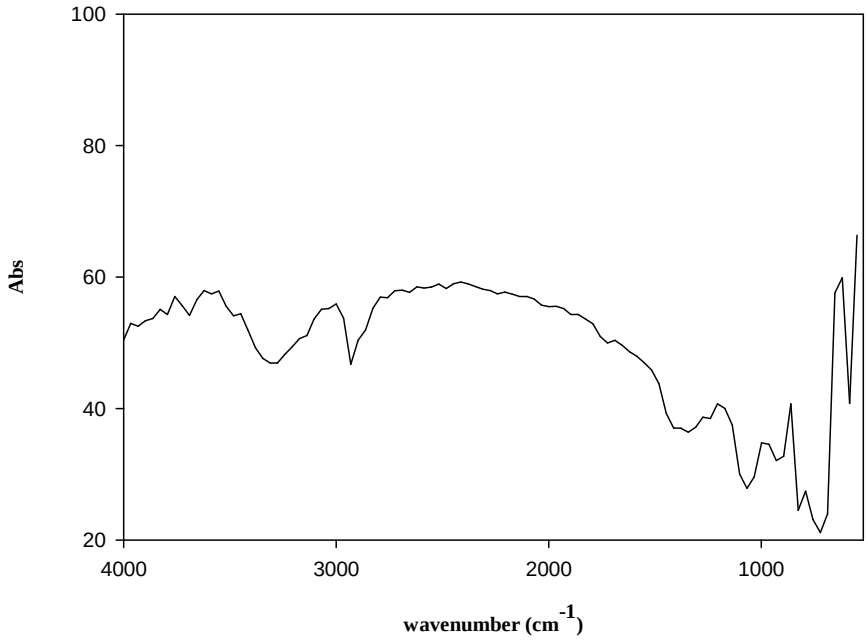

Figure 2. The FTIR spectrum of pure PVA.

Table 1. IR absorption bands and their assignment of pure PVA, compared with literatures.

Band position, cm^{-1}			Assignment
Present work	Literature		
3330	3500-3200	3360	OH stretching
2939	2920	2990	CH_2 asymmetric stretching
2866	-	2840	C–H symmetric stretching
1732	1720	1763	C=O stretching
1614	-	1650	C=O stretching
1533	-	1560	Conjugated C=C stretching
1430	1430	1436	CH_2 bending vibration
1341	1380	1348	C–H symmetric stretching
1238	-	1211	CH_2 wagging
1069	1140-1000	1031	C–O stretching vibrations
907		942	CH_2 rocking
833	850	879	C–C stretching
730		786	OH wagging
582		566	C–O bending vibrations

from alkene↔alkane and C=O↔C–O^- and presence of hydrogen bond with oxygen of C═O group (Abd El-Kader, 2003). Also, two absorption peaks were observed at 1430 and 1341 cm^{-1}. The absorption band at 1430 cm^{-1} is assigned as CH_2 bending vibration while the deformation vibration of C–CH_3 is associated with the absorption band at 1341 cm^{-1}. The absorption shoulder at 1238 cm^{-1} is arising from CH_2 wagging. Finally, the absorption band at 1069 cm^{-1} arises from the C–O stretching vibration while the band at 833 cm^{-1} results from C–C stretching vibration. CH_2 rocking was found at 907 and 730 cm^{-1} and OH wagging was found at 582 cm^{-1} (Ali et al., 2007).

FTIR spectroscopic analysis of gamma-irradiated pure PVA

The behavior of the irradiated PVA samples, up to 15, 25,

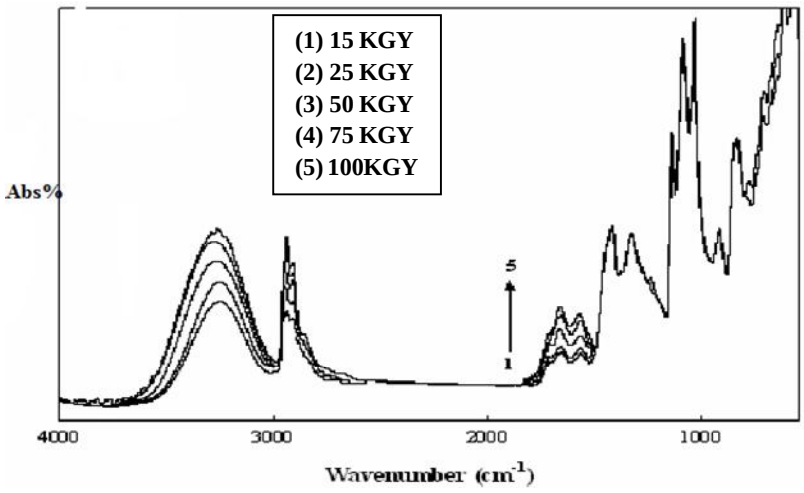

Figure 3. FTIR spectra of pure PVA, gamma-irradiated at different dose levels.

50, 75 and 100 kGy, were shown in Figure 3. Four remarkable changes were noticed here. The first is the feature in the -OH stretching vibration region. The 3330 cm^{-1} peak in the un-irradiated PVA become weaker as the irradiation dose increases and shifted to a lower wave number side. Secondly, the intensity of two strong bands at 2939 and 2866 cm^{-1} in un-irradiated PVA reduces markedly as the irradiation dose increases. Thirdly, the absorbance of stretching vibrational bands of C=O and C=C appeared at 1614 and 1533cm^{-1} were found to be positively changed as the irradiation dose was increased and are shifted to the higher side of the spectrum. Finally, the intensity of the absorption band at 1069 cm^{-1} was found to increase with increasing irradiation dose.

From FTIR analysis, it can be deduced that the decreasing intensity of the hydrogen-bonded-OH region may be attributed to the breaking of hydrogen bonds as a result of irradiation treatment which results in dehydration of the polymer matrix.

FTIR spectra of PVA/Ag nanocomposite samples

FTIR spectra of the PVA/Ag nanocomposites doped with different concentration of $AgNO_3$ gamma-irradiated at 25 kGy (a), 50 kGy (b), 75 kGy (c), and 100 kGy (d), as an example, were shown in Figure 4. Three structural features were induced due to interaction between Ag^+ ions and PVA chains. First, the –OH stretching band located at 3330 cm^{-1} was shifted to 3308 cm^{-1} and become to somewhat broader and weaker. It is well known that, when the metallic clusters and nanoparticles are capped by the PVA chains, two kinds of bonds may contribute to the Ag-PVA complication, namely, Ag–C and Ag–O bonds. The rigid structure of the C–C bond in monomer unit impedes the formation of Ag–C bonds. Hence, the binding of silver clusters by PVA is likely achieved through the Ag–O bond. The spectral shift together with reduced intensity of the –OH stretching vibration upon incorporation of the Ag nano-filler indicates to interaction between Ag nanoparticles and the OH groups originating from the PVA chains.

Second, the IR absorption band at 1614 cm^{-1} grew at the expense of the absorption band at 1533 cm^{-1} which was found to decay markedly with increasing $AgNO_3$ content. The increased intensity of the –C=O at 1614 cm^{-1} can be correlated to the prominent oxidative degradation reaction accompanying the reduction of Ag nanoparticles. The disappearance of 1533 cm^{-1} absorption peak can be attributed to some sort of –C=C– structure deformation and/or chain scissions of the polymer as a result of interaction with $AgNO_3$. Finally, the crystallization sensitive band at 1135 cm^{-1} was reduced as the $AgNO_3$ content was increased reflecting the negative effect of the $AgNO_3$ on the crystallinity of the PVA matrix. This result is in good agreement with the results obtained from XRD results (Tawfik et al., in press).

Effect of γ-rays on FTIR spectrum of nanocomposites

Figure 5 shows the FTIR spectra of PVA doped with 2, 4, 6 and 8 wt% $AgNO_3$, gamma-irradiated at 15, 25, 50, 75 and 100 kGy, as an example. From which, it is clear that the intensity of bands at 2939, 1732 and 833 cm^{-1} were observed to decrease further along with the disappearance of bands in the wave number region of 1250 to 1500 cm^{-1}, with increasing gamma dose. This indicates that gamma irradiation subsequently causes the structural rearrangements in PVA chains on embedding of Ag nanoparticles. These structural modifications in

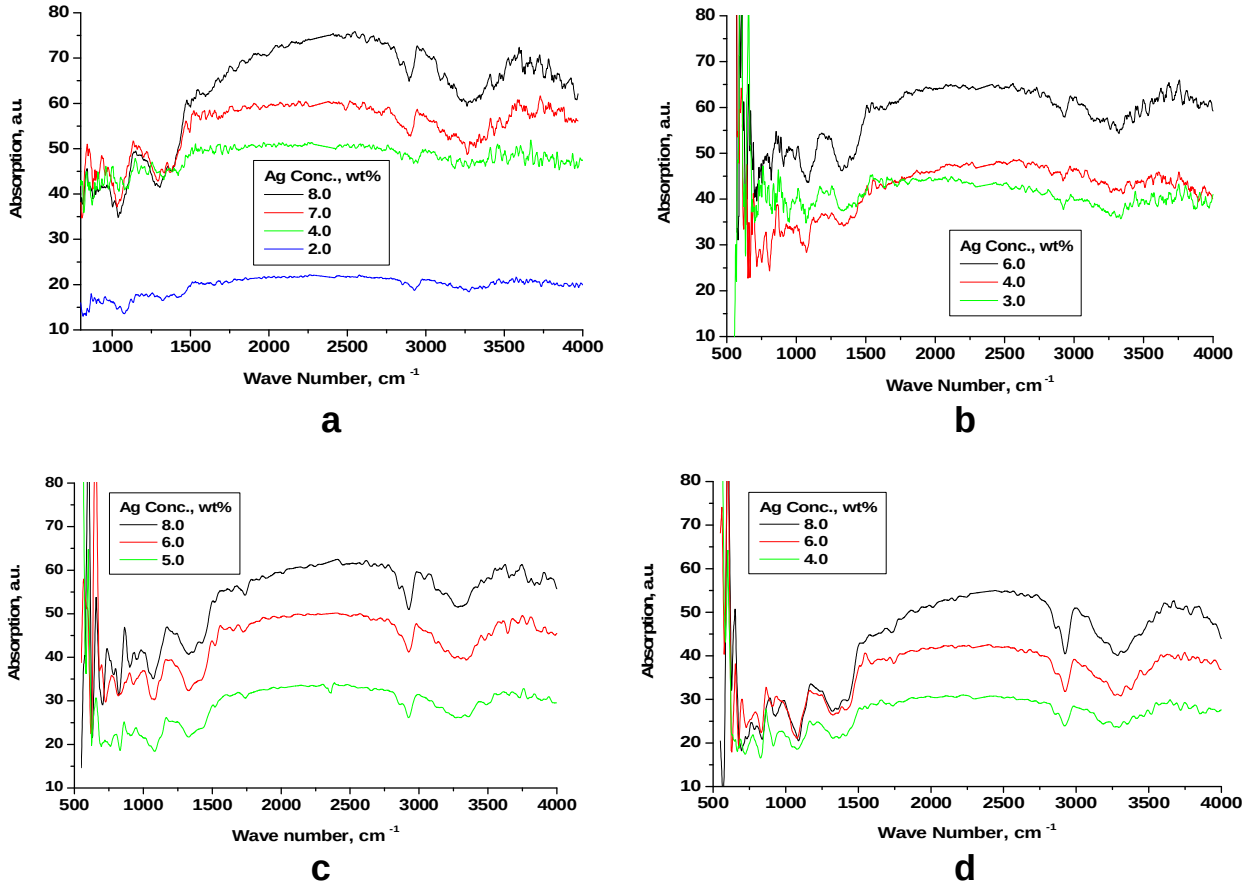

Figure 4. FTIR spectra of the PVA/Ag nanocomposites doped with different concentration of $AgNO_3$, γ-irradiated at 25 kGy (a), 50 kGy (b), 75 kGy (c), and 100 kGy (d).

host PVA matrix after embedding Ag nanoparticles and further, with exposure to gamma radiations, are in conformity with the observed changes in optical behavior (Tawfik et al., in press). The C=O stretching vibration intensity at 1614 cm^{-1} was increased as the irradiation dose increased. The loading of polymeric samples with $AgNO_3$ beside gamma-irradiation plays an important role for structural changes related to the enhancement in the degree of oxidation reaction. In this respect, it was found that the IR absorption bands associated with the oxidative degradation reaction increases whereas ones associated with cross-linking reaction totally decays.

DC-electrical characteristics of PVA/Ag nanocomposites

In general, the dc-electrical characteristic curves of the different nanocomposite samples were investigated, at room temperature. The investigated samples were divided into two groups: (a)- Samples fabricated with different $AgNO_3$ concentrations, at constant γ-irradiation dose, and (b)- Samples fabricated with constant $AgNO_3$ concentration, at different γ-irradiation doses. From which, the dc-conductivity (σ) could be calculated from the well known relationship:

$$\sigma = I \cdot L / V \cdot A \quad (1)$$

where:
I: Current,
V: Voltage,
L: Sample thickness, and
A: cross-sectional area of the electrode.

Effects of Ag concentration on the DC-electrical conductivity

Figure 6 shows the (I-V) characteristic curves of PVA/Ag nanocomposite prepared with different $AgNO_3$ concentration values of 2.0, 3.0, 4.0, 5.0, 6.0, 7.0 and 8.0 wt%, plotted at different gamma-irradiation dose levels of 15, 50, 75 and 100 kGy, as an example.

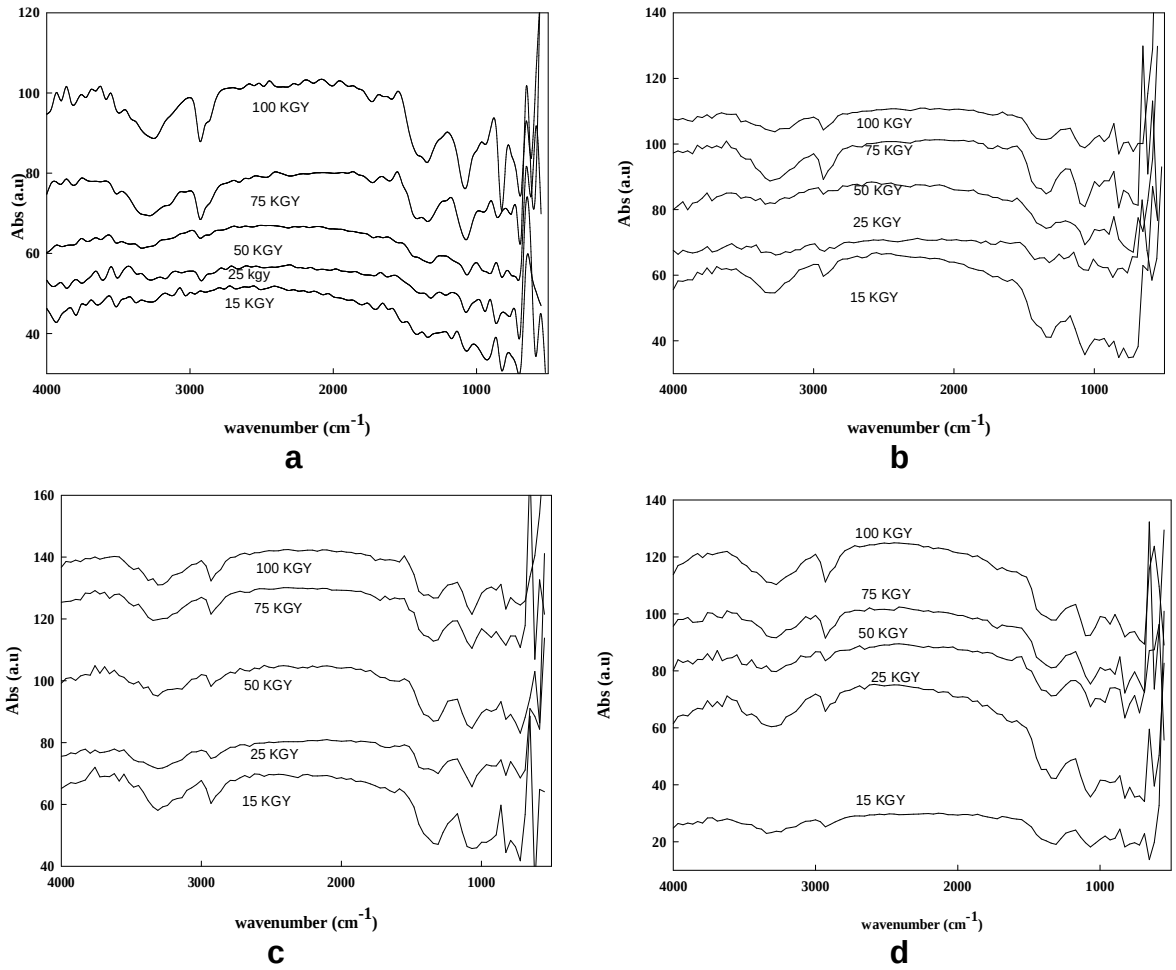

Figure 5. FTIR spectra of PVA/Ag doped at 2 wt % (a), 4 wt% (b), 6 wt% (c), and 8 wt% (d), gamma-irradiated with different dose levels.

The effect of $AgNO_3$ doping with different concentrations of 2.0, 3.0, 4.0, 5.0, 6.0, 7.0 and 8.0 wt% on the electrical conductivity of PVA films is shown in Figure 7. The room-temperature electrical conductivity showed a strong dependence on the concentration of the dopant ($AgNO_3$), with a maximum dependence value, for the sample doped with a concentration of 7 wt% of Ag. The conductivity of doped samples was shown to be always greater than that of the undoped samples. The observed effect of $AgNO_3$ doping on the electrical conductivity and conduction behavior of PVA films may be explained on the basis of charge transfer complex formation involving PVA molecules and the dopant Ag.

The formation of charge transfer complexes was also confirmed by the UV-Vis absorption studies made on $AgNO_3$ doped PVA films (Tawfik et al., in press). The increase in electrical conductivity for lower dopant concentration (2 wt%) may be explained on the basis of formation of charge transfer complexes which facilitates the delocalization of conduction electrons giving rise to higher conductivity. At higher concentration (8 wt%) of the dopant, however, the mobility of charge carriers decreases, mostly due to the segregation of dopant molecules (Uma Devi et al., 2002; Mustafa, 2013; Hadi et al., 2013; Mahendia et al., 2010).

From the obtained data, the electrical conductivity of PVA/Ag films was calculated, and plotted, for the fabricated samples, as a function of Ag concentrations (Figure 7). The dependence of the room-temperature electrical conductivity on Ag concentration follows a polynomial fit, following the equation:

$$Y = Y_o + B_1.X = B_2.X^2 \quad (2)$$

where:
Y_o and Y: initial value of conductivity, and value at certain Ag concentration,
B1 and B2: constants, and

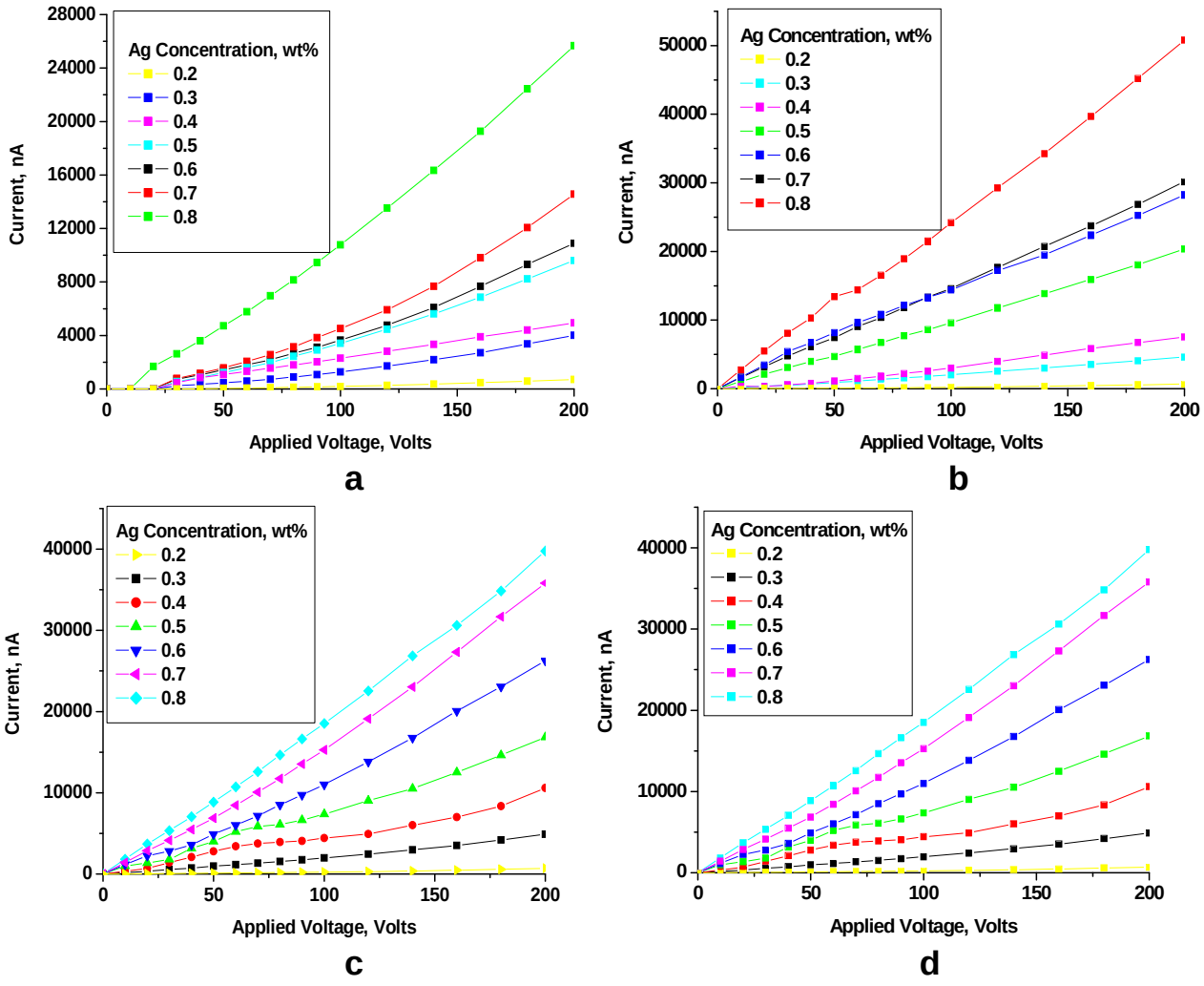

Figure 6. (I−V) characteristic curves of PVA/Ag nanocomposite fabricated with different $AgNo_3$ concentration, gamma-irradiated at 15 kGy (a), 50 kGy (b), 75 kGy (c), and 100 kGy (d).

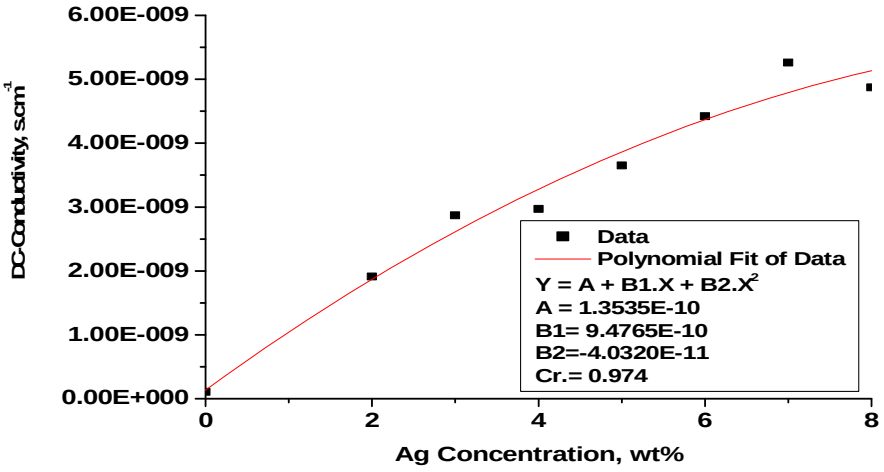

Figure 7. Dependence of the dc-conductivity (σ_{dc}) of PVA/Ag nanocomposites on concentration (wt%) of Ag nanoparticles.

X: Ag concentration.

Effect of gamma-irradiation on the electrical properties

The dependence of the dc-conductivity of the different samples on gamma-irradiation was studied in details. In this concern, the samples doped with (8 wt %) Ag nanoparticles were chosen as an example. In this concern, Figure 8 shows the variation of the dc-electrical conductivity of the samples doped at 8.0% on gamma-dose levels of 15, 25, 50, 75, and 100 kGy, as an example. From which, it is clear that the conductivity of PVA is decreased as the dose increased to 50 kGy. For higher dose levels, up to 100 kGy, the conductivity re-increase, again, up to around 6.5×10^{-9} S.cm^{-1}.

The obtained dependence may be due to cross-linking at the polymer chain. The inter-particle distance decreases as more Ag is incorporated and as the γ-dose increased, up to around 50 kGy, leading to decrease in the electrical conductivity of the PVA/Ag nanocomposites. For higher γ-dose levels, the conductivity re-increased, again. The matter is due to that Ag particle size increases again, which indicates chain scission in the (polymer) host matrix leading to increase in the conductivity. It was reported that the nanoparticles themselves could act as conductive junctions between the polymer chains that resulted in an increase of the electrical conductance of the composites (Gangopadhyay and Amitabha, 2000).

DC-conduction mechanism in PVA films doped with Ag

In order to study the dc-conduction mechanism in PVA films, a plot of log (I) versus log (V), for un-doped (Figure 9a) and Ag-doped PVA samples (Figure 9b) were plotted. In this concern, PVA/Ag samples irradiated with gamma dose of 25 kGy, were chosen, as an example. It is clearly shown that a linear dependence of log (I) on log (V) was obtained, confirming the relation $I \alpha V^m$, where m varying from m = 1, that is, the ohmic conduction, and m = 2, for the space charge conduction. That is, for the first condition (m = 1) obeys ohm's law (I α V) with slope ~ 1 whose terminal is usually called the trapping voltage (V_t).

The region in the (I−V) characteristic curves, which appears at low voltages, indicates that the current is controlled by generated carriers. The ohmic behavior can be understood on the basis of the reasonable assumption that at low voltages, there is no injection of carriers from the electrode contact, and the initial current is governed by the intrinsic free-carrier motion, that is, at the normal ranges of temperatures and pressures, the dominant charge carriers in a semiconductor are generated mainly by thermal excitation of the carriers. The Ag

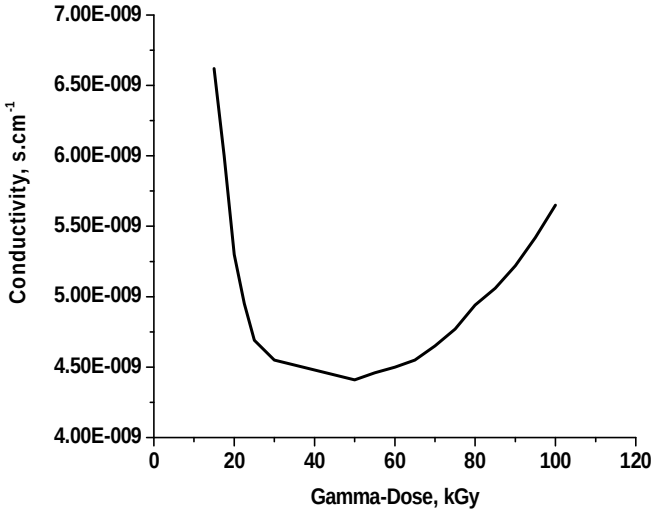

Figure 8. Dependence of dc-electrical conductivity on gamma-irradiation dose, for samples doped with Ag at 8.0 wt%.

semiconductor nanoparticles have a small energy band gap; hence, a small amount of energy is sufficient to excite electrons from full valence band to an upper empty conduction band.

In the second condition, at m = 2, at higher voltages, the current increases rapidly with applied voltage and the slope ~ 2, that is, the conduction becomes non ohmic. The results shown in Figure 9 need to be carefully analyzed, to identify the predominant conduction mechanism, since different types of conduction mechanisms can give rise to non-linear characteristics. The deviation of (I−V) characteristics of ohm's law can be explained considering various dc-electronic conduction mechanisms by which electrons are transported under the influence of an applied field. Tunneling, Schottky emission, Poole-Frankel emission, and Space Charge Limited Conduction (SCLC) are possible mechanisms for such a case. Generally, one mechanism will dominate the observed current but more than one conduction mechanisms may possibly operate at particular voltage value (Del Castillo-Castro et al., 2007; Nagraj et al., 2002). Here, it is worth noting that tunneling current originates only in very thin films. So, tunneling mechanism is excluded in the present case as the thickness is pretty high (1.0 mm).

To understand the actual conduction mechanism through the PVA/Ag nanocomposites, Poole–Frenkel or Richardson-Schottky mechanisms may be used to investigate the experimentally measured dependence of current on voltage in the high field region. The Poole–Frankel effect is associated with the excitation of carriers out of traps and the current is described by Geddes et al. (1990):

$$I \alpha \exp (e\beta v^{1/2}/kTd^{1/2}) \quad (3)$$

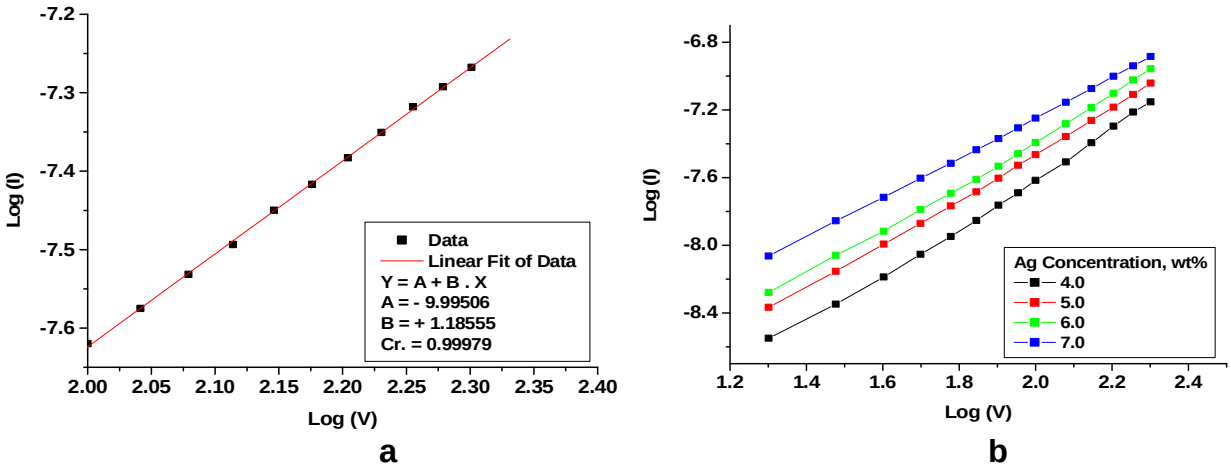

Figure 9. $\log_{10}$ (I) vs. $\log_{10}$ (V) plots for un-doped PVA films (a), and different PVA/Ag films, gamma-irradiated at 25 kGy (b).

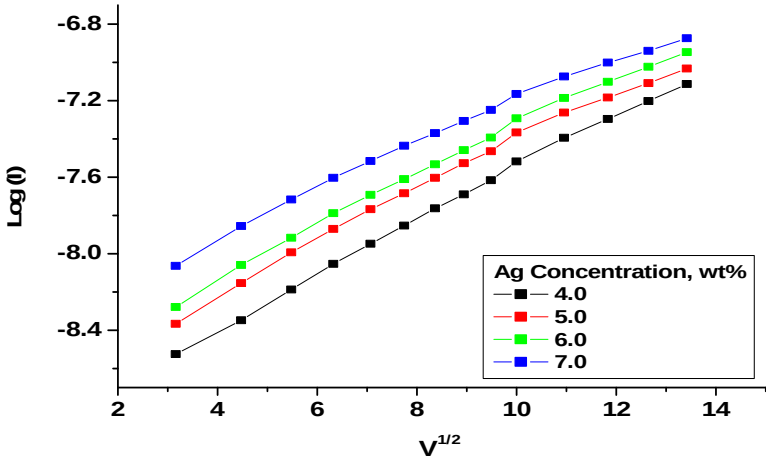

Figure 10. log (I) vs. $V^{1/2}$ of PVA/Ag nanocomposites with different concentrations of $AgNO_3$ (wt%), gamma-irradiated at 25 kGy.

where:
β_{PF}: Poole–Frenkel coefficient
V: applied voltage
K: Boltzmann's constant
T: absolute temperature
D: Sample thickness.

The theoretical value of β_{PF} is given by Hodge et al. (1996):

$$\beta_{pf} = (e^3 / \pi\ \varepsilon\varepsilon_0)^{1/2} \quad (4)$$

where, e is electronic charge, E is dielectric constant of PVA, and ε_o is free space permittivity.

On the other hand, the Schottky effect corresponds to the injection of carriers from the electrodes over the potential barrier formed at the semiconductor–metal interface, and the relationship between the pool frenkle coefficient and the Schottky coefficient described by Gould and Shafai (2000):

$$B_{RS} = 1/2\ \beta_{pf} \quad (5)$$

To decide whether the carriers are generated from the interior of the sample (Poole-Frenkel type), or injected from the metal electrode (Schottky type), in both cases a plot of log (I) vs.$V^{1/2}$ characteristic curves are expected to be linear in nature. In this concern, Figure 10 shows typical plots of log (I) versus $V^{1/2}$ for different samples with different concentrations of $AgNO_3$ in wt%. The almost linear relation of log (I) vs. $V^{1/2}$ suggests the electronic type conduction mechanism. The charge

Table 2. Theoretical and experimental values of β for undoped PVA and PVA/Ag doped with different concentration of Ag in (wt%), gamma-irradiated at 25 kGy.

Sample	Expriemental β_{exp} (*10^{-5}eV)	Theoretical β β_{RS} (*10^{-5}eV)	Theoretical β β_{pf} (*10^{-5}eV)
Undoped PVA	2.39000		
2Wt% Ag	2.35204		
3Wt% Ag	2.75730		
4Wt% Ag	2.78770	2.02934	4.05868
5Wt% Ag	2.79730		
6Wt% Ag	2.66842		
7Wt% Ag	2.58156		
8Wt% Ag	2.43814		

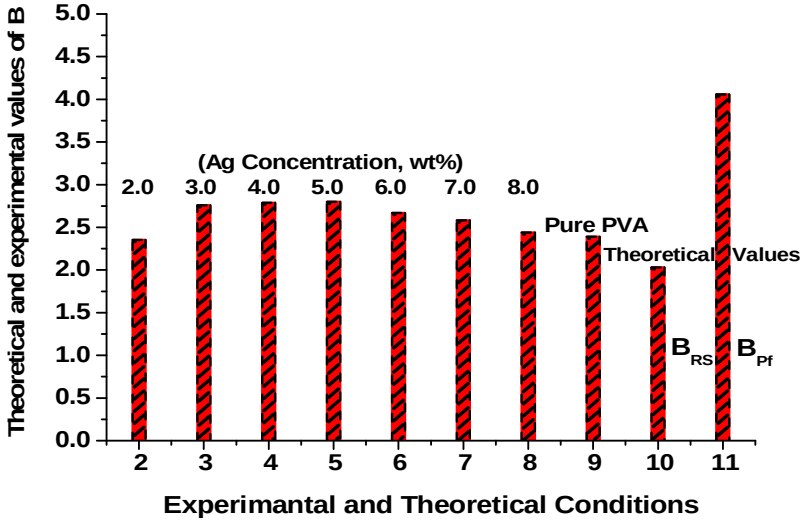

Figure 11. Histogram showing the theoretical and experimental values of β for different PVA films.

carriers are released by thermal activation over a potential barrier. To differentiate between these two mechanisms, the experimental values of β_{exp} for different Ag concentrations were determined from the slope of these plots and compared with theoretical values, as illustrated in Table 2 and shown in Figure 11.

It is clear from the figure that (current-voltage) characteristic curves for PVA/Ag films show a linear behavior with a slight deviation from linearity at higher voltages, which may be due to accumulation of space charge at the electrodes. The slopes of the linear regions on log (I) vs. $V^{1/2}$ relationships give information regarding the nature of the conduction mechanism operating in these films. Evaluation of the value of β_{exp} from these slopes suggests that Schottky emission is the dominant charge transport mechanism in films. Some results pointed out the Schottky emission (Kulanthaisami et al., 1995) as the dominant conduction mechanism in undoped and PVA/Ag films and some others attributed towards the Pool-Frenkle mechanism (Kulanthaisami et al., 1995). This discrepancy may be attributed to the difference in method of doping and film formation. Where, it is well known that both optical and electrical properties of PVA are strongly influenced by the dopant nature, the sample preparation method and environment.

CONCLUSIONS

From the study, experimental work, obtained results, analysis, it could be concluded that FTIR analysis indicated the formation of chemical bonding/conjugation between Ag nanoparticles and PVA chains. Whereas the effect of gamma-irradiation subsequently causes the structural rearrangements in PVA chains on embedding of Ag nanoparticles. Such induced structural changes

elucidate the observed behavior of these nanocomposites after gamma-irradiation. Also, the electrical performances of the PVA/Ag nanocomposites are greatly influenced by the concentration of the dopant Ag, and gamma-irradiation dose. As well, the obtained results corroborate towards the enhanced conducting behavior of PVA matrix with an increase in the concentration of embedded Ag nanoparticles. Finally, it is proved that Schottky emission is identified as the dominant conduction mechanism for dc conduction for both pure PVA and PVA/Ag films.

REFERENCES

Abd El-Kader KM, **2003**. Spectroscopic behavior of poly(vinyl alcohol) films with different molecular weights after UV irradiation, thermal annealing, and double treatment with UV irradiation and thermal annealing. J Appl Polym Sci, Vol. 88:589-594.

Ali Z, Youssef H, Afify T, **2007**. Structure-properties of electron beam irradiated and dicumyl peroxide cured low density polyethylene blends. Polym Comp, 105:2976-2980.

Ali ZI, Ali FA, Hosam AM, **2009**. Effect of electron beam irradiation on the structural xerogel. Spectro-chemica Acta, Part A, 72:868-875.

Del Castillo-Castro T, Larios-Rodriguez E, Molina-Arenas Z, Castillo-Ortega MM, Tanori J, **2007**. Synthesis and characterization of metallic nanoparticles and their incorporation into electroconductive polymer composites. Composites A: Appl Sci, 38:107-113.

Gangopadhyay R, **Amitabha** D, **2000**. Conducting polymer nanocomposites: A brief overview. Chem Mater, 12:608-622.

Geddes NJ, Sambles JR, Parker WG, Couch NR, Jarvis DJ, **1990**. Electrical characterisation of M/I/M structures incorporating thin layers of 22-tricosenoic acid deposited on noble metal base electrodes. J Phys D: Appl Phys, 23:95-102.

Ghanipour M, **Dorranian** D, **2013**. Effect of Ag-nanoparticles doped in polyvinyl alcohol on the structural and optical properties of PVA films. J Nanomater, 2013, Article ID 897043.

Gould RD, **Shafai** TS, **2000**. Conduction in lead phthalocyanine films with aluminium electrodes. Thin Solid Films, 373:89-93.

Hadi AG, Lafta F, Hashim A, Hakim H, Al-Zuheiry AIO, Salman SR, Ahmed H, **2013**. Study the effect of barium sulphate on optical properties of polyvinyl alcohol (PVA). Universal J Mat Sci, 1(2):52-55.

Hodge RM, Edward GH, Simon GP, **1996**. Water absorption and states of water in semicrystalline poly(vinyl alcohol) films. Polymer, 37:1371-1376.

Kulanthaisami S, Mangalaraj D, Narayandass SK, **1995**. Conduction studies on polyvinyl alcohol films. Eur Polym J, 31:969-975.

Mahendia S, Tomara AK, Kumar S, **2010**. Electrical conductivity and dielectric spectroscopic studies of PVA–Ag nanocomposite films. J Alloys Comp, 508:406-411.

Mohri N, Inoue M, Arai Y, Yoshikawa K, **1995**. Kinetic study on monolayer formation with 4-aminobenzenethiol on a gold surface. Langmuir, 11:1612-1616.

Mustafa FA, **2013**. Optical properties of NaI doped polyvinyl alcohol films. Phys Sci Res Int, 1(1):1-9.

Nagraj N, Reddy CVS, Sharma AK, Rao VVRN, **2002**. DC conduction mechanism in polyvinyl alcohol films doped with potassium thiocyanate. J Power Sources, 112:326-330.

Tawfik EK, Eisa WH, Mohamed RM, Fawzy YHA, El-Ghazaly MH, Ashry HA, **in press**. Gamma Radiation Synthesis and Characterization of PVA/Ag Nano-composite Films. J Radiat Res Appl Sci.

Uma Devi C, Sharama AK, Rao VVRN, **2002**. Electrical and optical properties of pure and silver nitrate-doped polyvinyl alcohol films. J Mat Lett, 56:167-174.

Citation: Tawfik EK, Fawzy YHA, M. H. El-Ghazaly MH, Ashry HA, 2015. Study of the DC-electrical properties of a novel polyvinyl alcohol/Ag hybrid nanocomposites. Phys Sci Res Int, 3(2): 26-36.